The neutrophil gelatinase-associated lipocalin (NGAL), a NF-κB-regulated gene, is a survival factor for thyroid neoplastic cells

Alessio Iannetti*†, Francesco Pacifico†‡, Renato Acquaviva*, Alfonso Lavorgna*, Elvira Crescenzi‡, Carlo Vascotto§, Gianluca Tell§, Anna Maria Salzano¶, Andrea Scaloni¶, Emilia Vuttariello‖, Gennaro Chiappetta‖ Silvestro Formisano*, and Antonio Leonardi*,**

*Dipartimento di Biologia e Patologia Cellulare e Molecolare, ''Federico II'' University of Naples, via S. Pansini 5, 80131 Naples, Italy; ‡Istituto di Endocrinologia ed Oncologia Sperimentale, via S. Pansini 5, 80131 Naples, Italy; §Dipartimento di Scienze e Tecnologie Biomediche, University of Udine, Piazzale Kolbe 4, 33100 Udine, Italy; ¶Laboratorio di Proteomica e Spettrometria di Massa, Istituto per il Sistema Produzione Animale in Ambiente Mediterraneo, Consiglio Nazionale delle Ricerche, via Argine 1085, 80147 Naples, Italy; and ‖Istituto Nazionale Tumori ''Fondazione G. Pascale'', via M. Semmola, 80131 Naples, Italy.

Edited by Guido Franzoso, Imperial College, United Kingdom, and accepted by the Editorial Board June 25, 2008 (received for review November 15, 2007)

NF-κB is constitutively activated in primary human thyroid tumors, particularly in those of anaplastic type. The inhibition of NF-κB activity in the human anaplastic thyroid carcinoma cell line, FRO, leads to an increased susceptibility to chemotherapeutic drug-induced apoptosis and to the blockage of their ability to form tumors in nude mice. To identify NF-κB target genes involved in thyroid cancer, we analyzed the secretome of conditioned media from parental and NF-κB-null FRO cells. Proteomic analysis revealed that the neutrophil gelatinase-associated lipocalin (NGAL), a protein involved in inflammatory and immune responses, is secreted by FRO cells whereas its expression is strongly reduced in the NF-κB-null FRO cells. NGAL is highly expressed in human thyroid carcinomas, and knocking down its expression blocks the ability of FRO cells to grow in soft agar and form tumors in nude mice. These effects are reverted by the addition of either recombinant NGAL or FRO conditioned medium. In addition, we show that the prosurvival activity of NGAL is mediated by its ability to bind and transport iron inside the cells. Our data suggest that NF-κB contributes to thyroid tumor cell survival by controlling iron uptake via NGAL.

Cancer is a multistep process during which cells undergo alterations of their normal functions that progressively lead to the genesis of a tumor. Among the most significant changes, cancer cells begin to secrete, into the tumor microenvironment, a number of factors that stimulate their own growth/survival and mediate angiogenesis and metastasis. During the last years, the role of NF-κB in the pathogenesis of human cancer has strongly emerged. In particular, because it is now generally accepted that chronic inflammation contributes to the genesis of many solid tumors, such as gastric, colon, or hepatic carcinomas, it has been recently shown that activation of NF-κB by the classical IKKβ-dependent pathway is a crucial mediator of inflammation-induced tumor growth and progression in animal models of inflammation-associated cancer (1, 2). This is not particularly surprising given that NF-κB controls expression of a number of proinflammatory factors (cytokines, chemokines ,and growth factors), secreted by cancer cells in the tumor microenvironment, that substantially contribute to tumor development (3, 4). Understanding the molecular mechanism by which these factors play their role in cancer could help in the comprehension of the role of NF-κB in inflammation-related cancer and could open innovative perspectives in the treatment of tumors.

We have shown that NF-κB is strongly activated in human anaplastic thyroid carcinomas (ATCs) (5). To study the role of NF-κB in thyroid cancer, we inhibited its function by stably transfecting FRO cells (derived from a human ATC) with a super-repressor form of IκBα (IκBαM). As a result, FRO IκBαM cells lost their oncogenic potential mainly from an increased susceptibility to drug-induced apoptosis (5).

The neutrophil gelatinase-associated lipocalin (NGAL), also known as lipocalin-2, is a member of a large family of lipocalins, a group of small extracellular proteins with great functional diversity (6). It is released from neutrophil granules as a 25-kDa monomer, a 46-kDa disulfide-linked homodimer, and a 135-kDa disulfide-linked heterodimer with a matrix metalloproteinase-9 (MMP-9) (7). NGAL is thought to be an acute phase protein (8) whose expression is up-regulated in human epithelial cells under different inflammatory conditions, such as inflammatory bowel disease (9). Elevated NGAL expression has also been shown in different human tumors including breast (10), lung (11), colon (9), ovary (12), and pancreas (13) carcinomas. However, the precise role of NGAL has not been well defined. Several studies have suggested that NGAL is a potent bacteriostatic agent that has siderophore-mediated sequestering of iron (14, 15), and that it is capable of protecting MMP-9 from autodegradation, thereby favoring the metastatic potential of cancer cells (16). As a secreted binding protein, it has been reported that the murine ortholog, 24p3, plays a crucial role in IL-3 deprivation-induced apoptosis by regulating intracellular iron delivery, very likely after interaction with a 24p3 receptor (17). Indeed, the human NGAL protects A459 and MCF7 cells from apoptosis induced by PDK1 inhibitors (18). Last, NGAL induces cell proliferation by promoting the iron-dependent metabolism of nucleotides for DNA synthesis (19).

The cellular system FRO/FRO IκBαM represents an excellent model for the identification of NF-κB-regulated factors that, when secreted in the extracellular milieu, could play a role in thyroid cancer. Thus, we used a different proteomic approach to analyze the pattern of expression of secreted proteins from conditioned medium of parental FRO cells and FRO IκBαM clones. One of the proteins that showed a marked decrease of expression in FRO IκBαM cells was NGAL. We show that knocking down NGAL expression blocks the ability of FRO cells to form colonies in soft agar and tumors in nude

Author contributions: A. Leonardi designed research; A.I., F.P., R.A., A. Lavorgna, E.C., C.V., A.M.S., and E.V. performed research; F.P., G.T., A.S., G.C., and S.F. analyzed data; and F.P. and A. Leonardi wrote the paper.

The authors declare no conflict of interest.

This article is a PNAS Direct Submission. G.F. is a guest editor invited by the Editorial Board.

†A.I. and F.P. contributed equally to this work.

**To whom correspondence should be addressed. E-mail: leonardi@unina.it

This article contains supporting information online at www.pnas.org/cgi/content/full/0710846105/DCSupplemental.

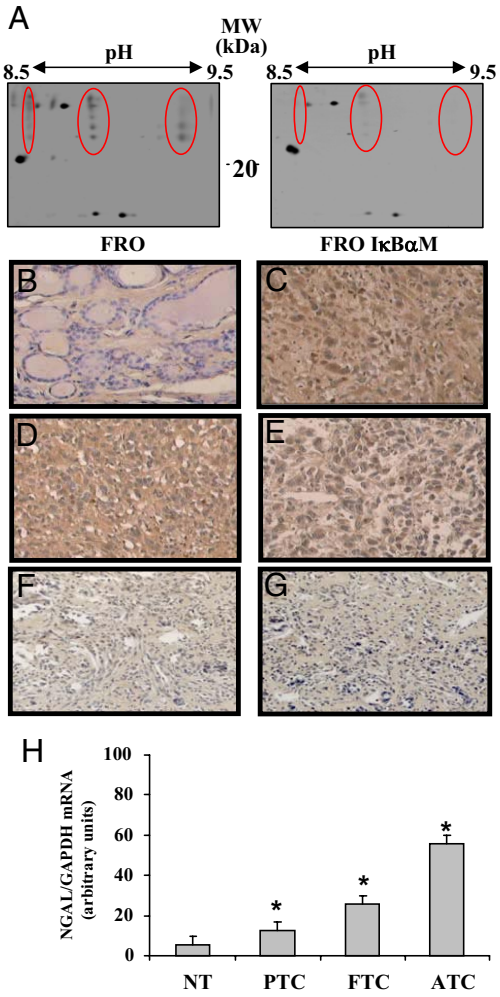

Fig. 1. Analysis of NGAL expression. Two-dimensional gel electrophoresis showing expression of NGAL in the conditioned medium of FRO IκBαM cells, as compared with parental counterpart FRO (*A*). Localization of NGAL *in situ* was determined by immunohistochemistry in sections from normal thyroid tissue (*B*) and three different ATCs (*C–E*). Lack of specific tissue staining was seen when either secondary Abs (*F*) or blocked Abs (*G*) were used. Magnification: ×400. (*H*) qRT-PCR analysis of NGAL mRNA levels in primary human cancers. NT, normal thyroid ($n = 2$); PTC, papillary thyroid carcinoma ($n = 3$); FTC, follicular thyroid carcinoma ($n = 3$); ATC, anaplastic thyroid carcinoma ($n = 3$). *, $P < 0.0005$.

mice and, therefore, increases their susceptibility to apoptosis. In addition, we show that the prosurvival activity of NGAL is mediated by its ability to bind and transport iron inside the cells.

Results

Differential Proteomic Analysis of Conditioned Media from FRO and FRO IκBαM Cell Lines. To identify factors secreted by thyroid cancer cells under transcriptional control of NF-κB, we analyzed the secretome of partially purified conditioned media from FRO and FRO IκBαM cell lines. Among the proteins whose expression decreased in the extracellular medium of FRO IκBαM cells, as compared with FRO, at least three groups were examined because of their strong reduction (Fig. 1 *A*, circled spots). The MALDI-TOF peptide mass fingerprint analysis identified all spots as NGAL, whose modifications after translation account for the multiple species that show variable molecular weight and pI values in the 2-DE gel.

Northern and Western blot assays confirmed the decreased expression of NGAL in FRO IκBαM cells, as compared with parental FRO cells [supporting information (SI) Fig. S1 *A–C*]. To confirm that NF-κB was controlling NGAL expression, we knocked down p65 expression in FRO cells by using siRNA and detected a decreased NGAL expression by Western blot analysis(Fig. S1*D*). In addition, WT and $p65^{-/-}$ mouse embryonic fibroblasts (MEF) were treated with IL1β or IL17, and the NGAL expression was detected by Northern and Western blot assays (Fig. S1 *E* and F). No induction of NGAL was detected in absence of p65. Reexpression of p65 in $p65^{-/-}$ MEF restored NGAL expression (Fig. S1*G*).

It was demonstrated that NF-κB controls NGAL expression via the inducible cofactor IκBζ (20, 21). We then investigated, by using chromatin immunoprecipitation, whether, in FRO cells, IκBζ was also bound to the NGAL promoter. As shown in Fig. S2, IκBζ was bound to the NGAL promoter together with the p50 and the p52 subunits of NF-κB.

Immunohistochemical Analysis of NGAL Expression in Normal and Pathological Human Thyroid Specimens. To verify the expression of NGAL in human primary thyroid cancer, we analyzed normal thyroid specimen and specimen from different thyroid carcinomas by immunostaining. As shown in Table 1 and Fig. 1 *B–G*, although NGAL expression was not detected in normal thyroid, NGAL immunostaining was positive for papillary, follicular and ATC. The levels of NGAL expression increased with the malignant phenotype of tumors, reaching the highest intensity in the anaplastic carcinomas (Table 1 and Fig. 1 *B–G*), in parallel with NF-κB basal activity in the same types of thyroid tumors (5). Real time PCR analysis confirmed the increased expression on the NGAL mRNA in primary human thyroid cancer (Fig. 1*H*).

Inhibition of NGAL Expression Leads to the Blockage of Tumorigenicity in FRO Cells. To study the role of NGAL in thyroid cancer, we blocked its expression in FRO cells by stable transfection of a siRNA targeting NGAL. Fig. 2*A* shows the levels of NGAL protein in two of the clones analyzed (indicated as siRNA NGAL 2/2 and 2/6) in FRO cells, either transfected with the empty vector (FRO Neo cells) or transfected with a control siRNA

Table 1. Immunohistochemical analysis of NGAL expression in normal and pathological human thyroid tissues

Histological type of thyroid samples	Number of total cases analyzed	Number of positive cases/ Number of total cases analyzed	NGAL staining score			
			0+	1+	2+	3+
Normal thyroid	3	0/3	3			
Papillary carcinoma	14	9/14	5	4	3	2
Follicular carcinoma	8	5/8	3		2	3
Anaplastic carcinoma	7	6/7	1		2	4

Human specimens were stained with anti-NGAL polyclonal antibodies. The percentage of malignant cells stained was scored from 0 to 3: 0, no positive cells; 1+, <10% of positive cells; 2+, 11–60% of positive cells; 3+, 61–100% of positive cells.

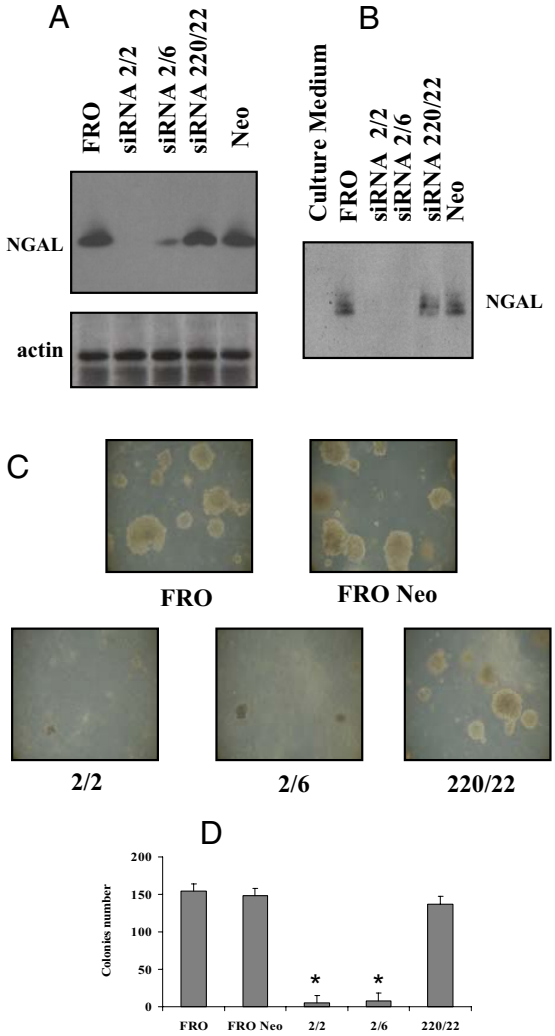

Fig. 2. Inhibition of NGAL expression by siRNA and *in vitro* oncogenic activity of the siRNA clones. The expression of NGAL in FRO cells, stably transfected with either siRNA plasmids (2/2, 2/6), control siRNA plasmid (220/22), or empty vector (Neo), was determined by Western blot analysis on total cell lysates (*A*) and on conditioned media (*B*). (*C*) Colony formation assay. Colonies >50 cells were scored after 2 weeks incubation at 37°C (*D*). Magnification: ×200. *, $P < 0.0001$ (2/2 and 2/6 vs. FRO, FRO-Neo, and 220/22).

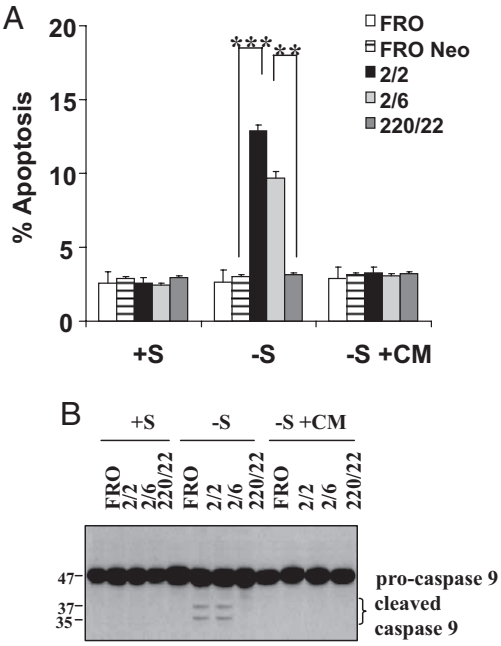

Fig. 3. NGAL protects FRO cells from apoptosis induced by serum-withdrawal. 2.5×10^5 cells per well were seeded in 6-well culture plates and grown either in the presence of serum (+*S*), in the absence of serum (−*S*), or in serum-free conditioned medium from FRO cells (−*S* + *CM*). Cell death was assessed by propidium iodide staining (*A*) and by Western blot analysis (*B*). Results were mean ± SD of at least three separate experiments. **, $P < 0.0005$; ***, $P < 0.0001$.

(indicated as siRNA NGAL 220/22). Fig. 2*B* shows the levels of secreted NGAL. These clones were tested for their ability to grow in semisolid medium and to form tumors in nude mice. In *in vitro* experiments, whereas FRO, FRO Neo, and 220/22 cells gave rise to foci of transformation, 2/2 and 2/6 clones did not form any colonies (Fig. 2 *C* and *D*). In *in vivo* assays, the injection of parental FRO or 220/22 cells into nude mice induced tumor formation in 12 of 12 mice, whereas the injection of 2/2 or 2/6 cells induced tumor formation in 1 of 6 and 4 of 6 mice, respectively (Table 2). The tumors developed from 2/2 and 2/6 cells were 4-fold and 2-fold smaller than those formed after injection of parental cells, respectively (Table 2). Notably, 2 of 4 tumors from 2/6 cells showed NGAL staining after immunohistochemical analysis, indicating that the expression of the siRNA plasmid was lost. We also blocked NF-κB in FRO cells by transient overexpression of IκBαM. In the absence of functional NF-κB, FRO cells did not form colonies in soft agar. Reexpression of NGAL partially rescued the ability of FRO cells to form colonies in soft agar (Fig. S3 *A–C*).

NGAL Is a Survival Factor in FRO Cells. We analyzed the response of parental FRO cells and NGAL siRNA clones to serum withdrawal-induced apoptosis. All clones grown in the presence of serum showed 2–3% apoptosis, as assessed by propidium iodide staining (Fig. 3*A*). Serum deprivation did not affect the survival of FRO, FRO Neo, and 220/22 clones but induced a significant cell death (10–15%) in 2/2 and 2/6 clones (Fig. 3*A*). This effect was reverted by the addition of the conditioned medium of either

Table 2. *In vivo* tumor growth induced by FRO Neo cells and FRO siRNA NGAL clones

Cell type	Tumor incidence	Tumor volume average, cm^3	Tumor weight average, g
FRO	6/6	0.37 ± 0.04	0.24 ± 0.05
FRO siRNA NGAL 2/2	1/6	0.01***	0.05***
FRO siRNA NGAL 2/6	4/6	0.16 ± 0.06**	0.11 ± 0.02**
FRO siRNA NGAL 220/22	6/6	0.33 ± 0.02	0.21 ± 0.03

2×10^7 cells were injected s. c. on a flank of each 6-week-old nude mouse. Tumor weight, diameter, and volume values were measured and determined as described in the *SI Text*. Two of four tumors developed by mice injected with FRO siRNA 2/6 cells showed partial NGAL staining after immunohistochemical analysis. ***, $P < 0.0001$ (FRO 2/2 vs. FRO); **, $P < 0.001$ (FRO 2/6 vs. FRO).

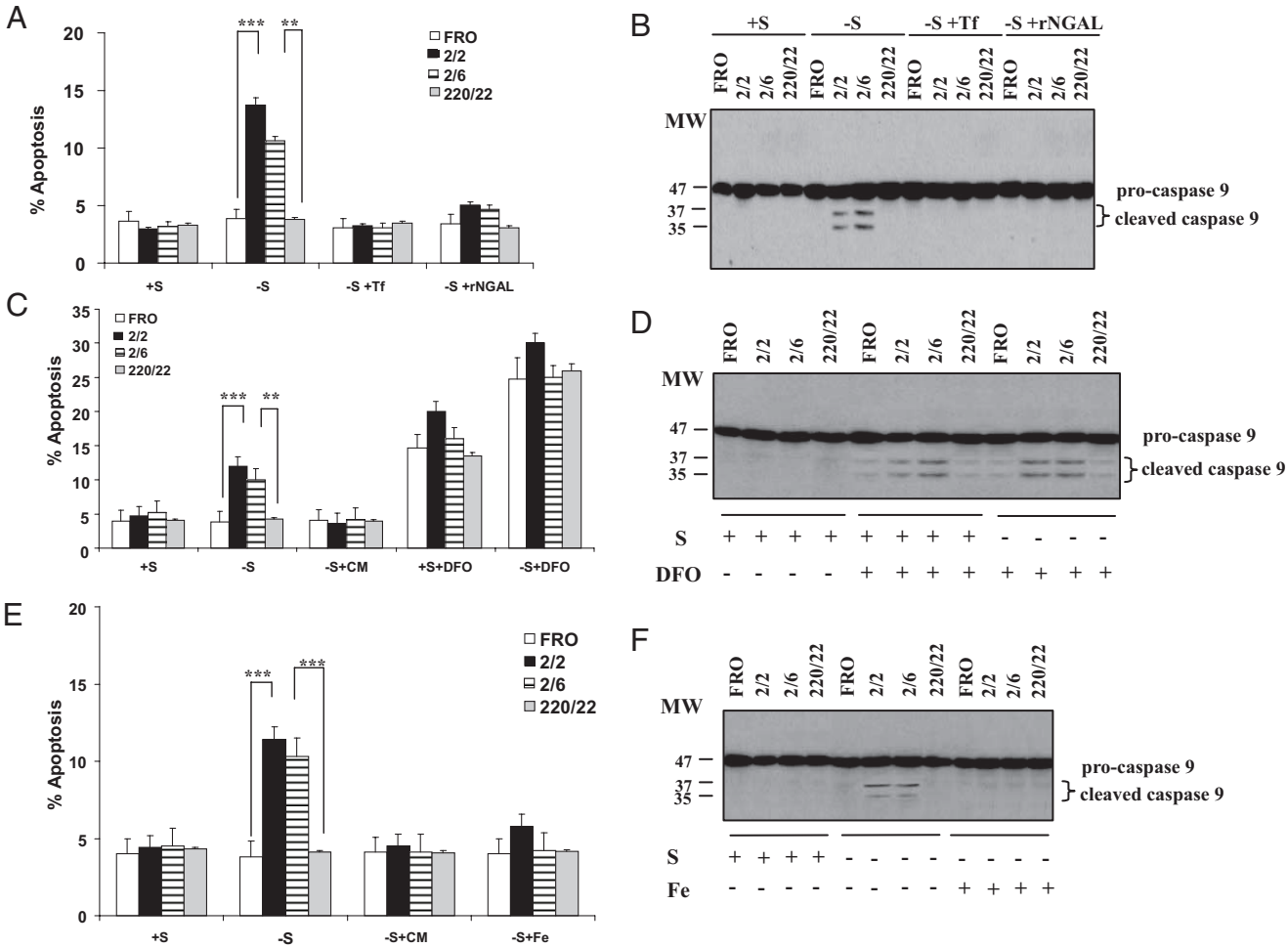

Fig. 4. Iron mimics the role of NGAL-mediated survival of FRO cells. 2.5×10^5 cells per well were seeded in 6-well culture plates and grown in different experimental conditions, as indicated. Cell death was either assessed by propidium iodide staining (*A*, *C*, and *E*) or by Western blot analysis (*B*, *D*, and *F*). Results were mean ± SD of at least three separate experiments. S, serum; CM, conditioned medium; Tf, transferrin; rNGAL, recombinant NGAL; DFO, deferoxamine; Fe, iron. **, $P < 0.0005$; ***, $P < 0.0001$.

FRO cells, FRO Neo cells, or 220/22 cells, to 2/2 and 2/6 clones. The same effect was also seen in the FRO cells transiently transfected with IκBαM (Fig. S3*D*). To confirm the activation of the apoptotic machinery, we analyzed by using Western blot analysis, the caspase-9 activity in parental FRO cells and NGAL siRNA clones grown in the same experimental conditions used in the propidium iodide assay (Fig. 3*B*). Serum deprivation induced cleavage of caspase-9 in 2/2 and 2/6 clones but not in parental FRO cells (Fig. 3*B*). Also, in this case, incubation of NGAL siRNA clones with the conditioned medium of FRO cells, FRO Neo cells, or 220/22 cells restored their survival (Fig. 3 *A* and *B*). These data strongly suggest that NGAL is a survival factor for thyroid carcinoma cells.

A dissection of the apoptosis pathways is illustrated in Fig. S4. In the NGAL siRNA clones grown in absence of serum, the initiating caspases-2 and -9 and the execution caspases-3 and 7 are activated, whereas the activity of other caspases (such as the initiating-, receptor-associated caspase-8) are not. This effect is reverted by the addition of either recombinant NGAL or iron (Fig. S4*A*). A very similar pattern of caspases activation is detected in FRO or 220/22 cells incubated with deferoxamine (DFO). Iron deprivation also resulted in the decrease of mitochondrial membrane potential (Fig. S4*B*) and in the release of cytochrome C (Fig. S4*C*). These data suggest that iron deprivation induces apoptosis via collapse of the mitochondrial membrane potential, release of cytochrome C from mitochondria, and activation of execution caspases.

NGAL-Mediated Intake of Extracellular Iron Accounts for the Antiapoptotic Activity of NGAL in FRO Cells. One of the properties of NGAL is an ability to deliver iron from the extracellular milieu into the cells. Because it has been described that iron could play an important role in cancer and apoptosis (22), we tested whether the increased susceptibility of siRNA NGAL clones to cell death was because of the decreased NGAL-mediated delivery of iron. We first analyzed the ability of iron-loaded transferrin and NGAL to rescue siRNA NGAL clones from serum deprivation-induced apoptosis. As reported in Fig. 4, both propidium iodide staining (*A*) and Western blot anti-caspase-9 (*B*) showed that addition of transferrin or recombinant NGAL to the serum-free medium restored the survival of siRNA clones.

To further confirm that NGAL acts as a survival factor for cancer cells by delivering iron, we used DFO (an iron chelator) and ferric chloride ($FeCl_3$, an iron source) to evaluate the survival of the siRNA clones. When cells were grown in complete medium in presence of DFO, both parental FRO cells and derived siRNA clones underwent apoptosis (Fig. 4 *C* and *D*). However, $FeCl_3$ produced the opposite effect; it restored the resistance of siRNA NGAL clones to serum deprivation-induced apoptosis (Fig. 4 *E* and *F*).

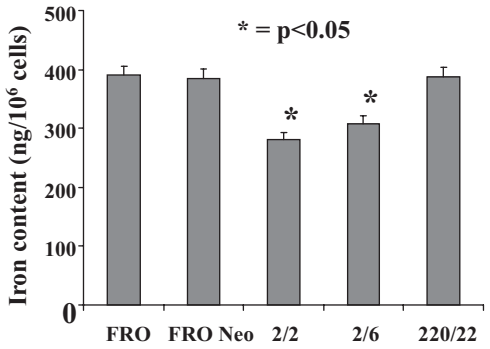

Fig. 5. Intracellular iron content of the different FRO cell lines. Colorimetric analysis of intracellular iron concentration is shown. Results were mean ± SD of at least three separate experiments, performed in triplicate. Significantly different from controls. *, $P < 0.05$.

Because these results indicated that the intracellular iron content could be relevant for the survival of FRO cells, we analyzed the intracellular iron concentration of parental FRO cells and NGAL siRNA clones (Fig. 5). The colorimetric assay showed that 2/2 and 2/6 clones lacked at least 20–30% of iron content ($P < 0.05$) compared with FRO, FRO Neo, and 220/22 cells, thus suggesting that the absence of NGAL determined a decrease of iron uptake in the clones.

Discussion

We have identified NGAL as a mediator of the NF-κB oncogenic activity in thyroid cancer. NGAL is highly expressed in the human thyroid carcinoma FRO cell line and other poorly differentiated thyroid cancer cell lines (Fig. 1*A* and data not shown), is highly expressed in primary human ATC (Fig. 1 *B–E* and Table 1), and acts as a survival factor for thyroid cancer cells (Figs. 3 and 4). The prosurvival activity of NGAL is mediated by its ability to bind iron and to transport it inside the cells (Figs. 4 and 5). These findings show that NGAL is a critical effector of NF-κB-mediated oncogenic activity, defines a prosurvival function of NGAL, and highlights iron as a central controller of cell survival.

Various types of cancers express high levels of NGAL, including colon, pancreas, breast, bladder, and liver (9–13). NGAL represents the human homolog of the rat neu-related lipocalin, a gene that was shown to be overexpressed in HER-2/neu oncogene-induced rat mammary tumors (23). Whether NGAL is causal or contributory to cancer is unknown. It has been reported that NGAL is a surviving factor for cancer cells. Ectopic expression of NGAL in lung and breast cancer cell lines reduced the apoptosis that was induced by a PDK1 inhibitor whereas the decreased expression of NGAL by siRNA had opposite effects (18). Our results confirm that NGAL is a surviving factor for cancer cells, and we extend these findings by demonstrating that the protective effect of NGAL is mediated by its ability to bind and transport iron. Our results are in agreement with the model proposed by Devireddy *et al.* (17). In this model, it is proposed that internalization of the apo form of NGAL leads to iron loss and apoptosis. Conversely, internalization of iron-loaded NGAL might prevent apoptosis.

Iron contributes to enzyme activity in DNA synthesis, metabolism, and oxygen response, and its acquisition plays a critical role in development, cell growth, and survival (22). Cancer cells have a higher requirement for iron than normal cells because they rapidly proliferate. This is reflected by the evidence that tumor cells have higher numbers of transferrin receptors on their surface, mediating a high rate of iron uptake (24). The importance of keeping the levels of iron uptake constant is further suggested by the evidence that multiple and redundant systems for iron uptake and transport exist. Most cells acquire iron by capturing iron-loaded transferrin. However, hypotransferrinemic mice (25, 26) and humans (27) have defects in central nervous system development and hematopoiesis when most epithelial organs are normal. Likewise, the mice lacking the transferrin receptor 1 initiate organogenesis but succumb to the effects of anemia (28). Given that iron is necessary for all of the cells, there must be other pathways for iron acquisition in epithelial cells. One such pathway is mediated by NGAL. In our experimental model, we observed that cells knocked down for NGAL expression showed a decrease of ≈20–30% iron content, and that this decrease still allowed cell survival. However, whether either the iron delivery was further decreased or cells were exposed to an appropriate stress, such as serum deprivation, cells underwent apoptosis. Indeed, administration of iron, either as iron salt, transferrin, or iron-loaded NGAL, restored the ability of knockdown cells to survive in the absence of serum. Similarly, NGAL knockout mice are vital and do not show gross developmental defects, although they succumb to bacterial infection (29).

Many studies have demonstrated that iron chelators, such as DFO, have effective anticancer activity (30). Iron is essential for the catalytic activity of ribonucleotide reductase (an enzyme mediating the conversion of all four ribonucleotides to their deoxyribonucleotide counterparts), which is the rate-limiting step of DNA synthesis (31). However, in our experimental system, the proliferation rate of the cells knocked down for NGAL expression is not affected (data not shown).

Iron levels strictly control the activity of specific prolyl hydroxylase-domain enzymes (PHDs), which, in turn, promote functional activation of transcription factors involved in tumor development, as is the case of the HIF-1, which controls genes involved in energy metabolism and angiogenesis (32). HIF-1 is primarily regulated by specific PHDs that initiate its degradation via the von Hippel-Lindau tumor suppressor protein. The oxygen and iron dependency of PHD activity accounts for regulation of the pathway by both cellular oxygen and iron status. We have evidence that in our experimental system, the protein level of HIF-1α is increased in the NGAL knockdown clones and is down-regulated by the addition of iron. Conversely, in control cells, the level of HIF-1α protein is low and up-regulated by the addition of DFO. Moreover, the activity of a HIF1-responsive promoter parallels the level of HIF-1 protein (A.I., F.P., and A. Leonardi, unpublished observation). Because NF-κB is a central component in the hypoxic response that positively regulates HIF-1α expression (33), it is tempting to speculate that the involvement of NGAL as an iron transporter, and its opposing effect on HIF-1α expression, could be a part of an autoregulatory loop that has inhibitory function between NF-κB and HIF-1 to control tumor progression.

Modulation of cell survival may not be the only way NGAL influences the behavior of a cancer cell. NGAL has been demonstrated to form a complex with MMP-9, playing a role in the maintenance of an extracellular pool of a potentially active form of the protease, whose activity is associated with angiogenesis and tumor growth (16). This is supported by the evidence that the level of NGAL expression correlates with the clinical outcome of the patients and the depth of the tumor invasion (17). We have evidence that a complex between NGAL and MMP-9 also exists in transformed thyroid cells, although neither the exact role that such a complex plays in thyroid cancer, nor whether or not the activity of MMP-9 is affected by the presence of NGAL, is known (A.I. and A. Leonardi, unpublished observations).

In other experimental systems, NGAL has been shown to induce expression of E-cadherin to promote formation of polarized epithelia and diminish invasiveness of ras-transformed

cell lines (34). In our experimental system, NGAL seems to have a different role. In fact, ectopic expression of NGAL in a normal thyroid cell line, or its knockdown in transformed cells, does not alter the expression of E-cadherin or vimentin (data not shown).

Our results, in addition to identifying NGAL as a potential target for therapeutic intervention, also strengthen the rationale for the use of iron chelators in the treatment of cancer. Depleting iron from a rapidly dividing cancer cell through the implementation of iron chelators, or decreasing NGAL expression, deprives iron of a component critical for various cellular processes and induces apoptosis.

Materials and Methods

Cell cultures and biological reagents, processing of conditioned media, two-dimensional gel elecrophoresis, mass spectrometry analysis, immunohistochemical analysis, Northern and Western blot experiments, *in vitro* and *in vivo* tumorigenicity assays, measurements of apoptosis, quantification of iron content, and statistical analysis were performed as described in the *SI Text*.

ACKNOWLEDGMENTS. This work was supported by Ministero dell'Istruzione, dell'Universita e della Ricercà, Fondo per gli Investimenti della Ricerca di Base Grant RBRN07BMCT (to G.T.) and a grant from the Associazione Italiana Ricerca sul Cancro (A.L.).

1. Greten FR, *et al.* (2004) IKKbeta links inflammation and tumorigenesis in a mouse model of colitis-associated cancer. *Cell* 118:285–296.
2. Pikarsky E, *et al.* (2004) NF-kappaB functions as a tumour promoter in inflammation-associated cancer. *Nature* 431:461–466.
3. Karin M (2006) Nuclear factor-kappaB in cancer development and progression. *Nature* 441:431–436.
4. Lin WW, Karin M (2007) A citokine-mediated link between innate immunity, inflammation, and cancer. *J Clin Invest* 117:1175–1183.
5. Pacifico F, *et al.* (2004) Oncogenic and anti apoptotic activity of NF-κB in human thyroid carcinomas. *J Biol Chem* 279:54610–54619.
6. Flower DR, North AC, Sansom CE. (2000) The lipocalin protein family: Structural and sequence overview. *Biochim Biophys Acta.* 1482:9–24.
7. Kjeldsen L, Johnsen AH, Sengeløv H, Borregaard N (1993) Isolation and primary structure of NGAL, a novel protein associated with human neutrophil gelatinase. *J Biol Chem* 268:10425–10432.
8. Nilsen-Hamilton M, *et al.* (2003) Tissue involution and the acute phase response. *Ann N Y Acad Sci* 995:94–108.
9. Nielsen BS, *et al.* (1996) Induction of NGAL synthesis in epithelial cells of human colorectal neoplasia and inflammatory bowel diseases. *Gut* 38:414–420.
10. Stoesz SP, *et al.* (1998) Heterogeneous expression of the lipocalin NGAL in primary breast cancers. *Int J Cancer* 79:565–572.
11. Friedl A, Stoesz SP, Buckley P, Gould MN (1999) Neutrophil gelatinase-associated lipocalin in normal and neoplastic human tissues. Cell type-specific pattern of expression. *Histochem J* 31:433–441.
12. Bartsch S, Tschesche K (1995) Cloning and expression of human neutrophil lipocalin cDNA derived from bone marrow and ovarian cancer cells. *FEBS Lett* 357:255–259.
13. Furutani M, Arii S, Mizumoto M, Kato M, Imamura M (1998) Identification of a neutrophil gelatinase-associated lipocalin mRNA in human pancreatic cancers using a modified signal sequence trap method. *Cancer Lett* 122:209–214.
14. Goetz DH, *et al.* (2002) The neutrophil lipocalin NGAL is a bacteriostatic agent that interferes with siderophore-mediated iron acquisition. *Mol Cell* 10:1033–1043.
15. Flo TH, *et al.* (2004) Lipocalin 2 mediates an innate immune response to bacterial infection by sequestrating iron. *Nature* 432:917–921.
16. Fernández CA, *et al.* (2005) The matrix metalloproteinase-9/neutrophil gelatinase-associated lipocalin complex plays a role in breast tumor growth and is present in the urine of breast cancer patients. *Clin Cancer Res* 11:5390–5395.
17. Devireddy LR, Gazin C, Zhu X, Green MR (2005) A cell-surface receptor for lipocalin 24p3 selectively mediates apoptosis and iron uptake. *Cell* 123:1293–1305.
18. Tong Z, *et al.* (2005) Neutrophil gelatinase-associated lipocalin as a survival factor. *Biochem J* 391:441–448.
19. Le NT, Richardson DR (2002) The role of iron in cell cycle progression and the proliferation of neoplastic cells. *Biochim Biophys Acta* 1603:31–46.
20. Cowland JB, Sorensen OE, Sehested M, Borregaard N (2003) Neutrophil Gelatinase Associated Lipocalin is up-regulated in human epithelial cells by IL-1β, but not TNF-α. *J Immunol* 171:6630–6639.
21. Cowland JB, Muta T, Borregaard N (2006) Neutrophil Gelatinase Associated Lipocalin is controlled by IκBζ. *J Immunol* 176:5559–5566.
22. Dunn LL, Rahmanto YS, Richardson DR (2007) Iron uptake and metabolism in the new millennium. *Trends Cell Biol* 17:93–100.
23. Stoesz SP, Gould MN (1995) Overexpression of neu-related lipocalin (NRL) in neu-initiated but not ras or chemically initiated rat mammary carcinomas. *Oncogene* 11:2233–2241.
24. Richardson DR, Ponka P (1997) The molecular mechanisms of the metabolism and transport of iron in normal and neoplastic cells. *Biochim Biophys Acta* 1331:1–40.
25. Huggenvik JI, *et al.* (1989) A splicing defect in the mouse transferrin gene leads to congenital atransferrinemia. *Blood* 74:482–486.
26. Trenor CC, III, Campagna DR, Sellers VM, Andrews NC, Fleming MD (2000) The molecular defect in hypotransferrinemic mice. *Blood* 96:1113–1118.
27. Hayashi A, Wada Y, Suzuki T, Shimizu A (1993) Studies on familial hypotransferrinemia: Unique clinical course and molecular pathology. *Am J Hum Genet* 53:201–213.
28. Levy JE, Jin O, Fujiwara Y, Kuo F, Andrews NC (1999) Transferrin receptor is necessary for development of erythrocytes and the nervous system. *Nat Genet* 21:396–399.
29. Berger T, *et al.* (2006) Lipocalin 2-deficient mice exhibit increased sensitivity to Escherichia coli infection but not to ischemia-reperfusion injury. *Proc Natl Acad Sci USA* 103:1834–1839.
30. Buss JL, Torti FM, Torti SV (2003) The role of iron chelation in cancer therapy. *Curr Med Chem* 10:1021–1034.
31. Richardson DR (2005) Molecular mechanisms of iron up-take by cells and the use of iron chelators for the treatment of cancer. *Curr Med Chem* 12:2711–2729.
32. Semenza G (2001) HIF-1, O2, and the 3 PHDs: How animal cells signal hypoxia to the nucleus. *Cell* 107:1–3.
33. Rius J, *et al.* (2008) NF-κB links innate immunity to the hypoxic response through transcriptional regulation of HIF-1α. *Nature* 453: 807–811.
34. Hanai J, *et al.* (2005) Lipocalin 2 diminishes invasiveness and metastasis of Ras-transformed cells. *J Biol Chem* 280:13641–13647.

Supporting Information

Iannetti *et al.* 10.1073/pnas.0710846105

SI Text

Cell Culture and Biological Reagents. FRO, FRO IκBαM, and FRO siRNA NGAL were grown in DMEM (Sigma), supplemented with either 10% FBS (Sigma) or OPTIMEM (Invitrogen), and either supplemented or not with 10% FBS (Sigma). Human neutrophil gelatinase-associated lipocalin (NGAL) was amplified by PCR from a human liver c-DNA library (Clontech) and cloned into pcDNA3.1-HA, -FLAG vectors (Invitrogen) for expression in mammalian cells and into pET28 (Novagen) for expression in *Escherichia coli*. Human transferrin was from Kedrion. Anti-NGAL (AF1757) and anti-actin (sc-8432) antibodies were purchased from R&D Systems and Santa Cruz Biotechnology, respectively. A polyclonal rabbit anti-NGAL antibody was generated in rabbits by using human recombinant NGAL protein as an antigen. IL1β and IL17 were from Peprotech and Biosource, respectively. Transient transfection of FRO cells was performed by using the Nucleofector™ (Amaxa).

Processing of Conditioned Media. Conditioned media (1 liter) from FRO and FRO IκBαM cell lines, and grown in OPTIMEM without serum, were collected and centrifuged at 1500 × *g* for 10 min at 4°C to remove cells and cell debris. The samples were concentrated to 5 ml over a membrane pressure concentrator with a 50-kDa cut-off (Millipore) and partially purified by using Mono-Q and Mono-S Econo-Pac columns (Bio-Rad).

Two-dimensional Gel Electrophoresis (2-DE) Analysis. The analysis was performed in triplicate on protein preparations from three different batches of conditioned media. Thirty–fifty μg of proteins were loaded onto 13-cm, pH 3–10 L, 4–7 L, or 6–11 L IPG strips (Amersham Pharmacia Biosciences). Isoelectro focusing was performed by using an IPGPhor II system (Amersham Pharmacia Biosciences) according to the manufacturer's instructions. Focused strips were equilibrated with 6.0 M urea, 26 mM DTT, 4% (wt/vol) SDS, and 30% (vol/vol) glycerol in 0.1 M Tris·HCl (pH 6.8) for 15 min, followed by 6.0 M urea, 0.38 M iodoacetamide, 4% (wt/vol) SDS, 30% (vol/vol) glycerol, and a dash of bromophenol blue in 0.1 M Tris·HCl (pH 6.8) for 10 min. The equilibrated strips were applied directly to SDS-10% (wt/vol) polyacrylamide gels and separated at 130 V. Gels were fixed and stained with ammoniacal silver (6). Gels were scanned with an Image Master 2-D apparatus and analyzed by Melanie 5 software (Amersham Pharmacia Biosciences), which allows estimation of relative differences in spot intensities for each represented protein. Statistical analysis of differentially expressed proteins was performed as described (4, 5).

Mass Spectrometry Analysis. Spots from 2-DE were excised from the gel, triturated, and washed with water. Proteins were *in-gel* reduced, S-alkylated, and digested with trypsin as reported (4, 5). Digested aliquots were removed and subjected to a desalting/concentration step on μZipTipC$_{18}$ (Millipore) by using acetonitrile as eluent before MALDI-TOF-MS analysis. Peptide mixtures were loaded on the MALDI target by using the dried droplet technique and α-cyano-4-hydroxycinnamic acid as the matrix and analyzed by using a Voyager-DE PRO mass spectrometer (Applied Biosystems). Internal mass calibration was performed with peptides derived from trypsin autoproteolysis. The PROWL software package was used to identify spots unambiguously (estimated Z-score >2) from independent, nonredundant, sequence databases (7). Candidates from peptide matching analysis were further evaluated by comparison with their calculated mass and pI by using the experimental values obtained from 2-DE.

siRNA of NGAL. To knock down NGAL expression, we designed double-stranded oligonucleotides, containing sequences derived from the human NGAL (nucleotides 294–313 and 376–397), in forward and reverse orientation, and separated them by a 7-bp spacer region (caagaga) to allow the formation of the hairpin structure in the expressed siRNAs. NGAL siRNA 220: sense strand, 5′ –CCATCTATGAGCTGAAAGAcaagagaTCTTTCAGCTCATAGATGG; antisense strand, 5′ – CCATCTATGAGCTGAAAGAtctcttgTCTTTCAGCTCATAGATGG. NGAL siRNA 2; sense strand, 5′ – GGACTTTTGTTCCAGGTTGTTcaagagaAACAACCTGGAACAAAAGTCC; and antisense strand, 5′ – GGACTTTTGTTCCAGGTTGTTtctcttgAACAACCTGGAACAAAAGTCC. The resulting double-stranded oligonucleotides were cloned into the pcRNAi vector that we derived from the pcDNA3.1 vector (Invitrogen) by replacing the viral promoter-cassette with the H1 promoter that is specifically recognized by RNA polymerase III (2).

Quantification of Iron Content by Colorimetric Assay. Cell cultures in 100-mm dishes were washed twice with PBS and then lysed in 400 μl of 50 mM NaOH for 2 h on a shaker in a humidified atmosphere. The lysates were incubated for 20 min at room temperature in 0.3 M HCl, TCA-precipitated, and finally centrifuged at 1200 g for 15 min. The supernatants were mixed with chromogen (0.51 mM disulphonate bathophenantroline, 1.3 M sodium acetate, pH 4.6, 30 mM sodium pyrosulphite, and 1.83 mM p-(N-methyl)aminophenol), and the absorbance was spectrophotometrically determined at the wavelength of 546 nm. This method was also used to confirm the presence of iron in both human transferrin and recombinant NGAL.

Immunoistochemical Analysis. Specimens from normal and pathological human thyroid were isolated, rinsed with PBS, fixed in 4% buffered neutral formalin, and embedded in paraffin. Then, 5–6-μm thick paraffin sections were deparaffinized, placed into a solution of absolute methanol and 0.3% hydrogen peroxide for 30 min, and then washed in PBS before immunoperoxidase staining. Slides were then incubated overnight at 4°C in a humidified chamber with antibody anti-NGAL diluted 1:100 in PBS and subsequently incubated, first with biotinylated goat anti-rabbit IgG for 20 min (Vectostain ABC kits, Vector Laboratories) and then with premixed reagent ABC (Vector) for 20 min. The antibody anti-NGAL was a rabbit polyclonal raised against the recombinant NGAL protein. The immunostaining was performed by incubating slides in diaminobenzidine (DAB-DAKO) solution containing 0.06 mM DAB and 2 mM hydrogen peroxide in 0.05% PBS, pH 7.6, for 5 min. After chromogen development, slides were washed, dehydrated with alcohol and xylene, and mounted with coverslips by using a permanent mounting medium (Permount). As a control of the immune reaction, slides were incubated with an anti-NGAL Ab previously incubated with recombinant NGAL (1 mg/ml).

Northern and Western Blots. For Northern blot, 20 μg of total RNA from FRO and FRO IκBαM cell lines was analyzed by electrophoresis on a 1.2% formaldehyde agarose gel and blotted onto nitrocellulose membrane (Bio-Rad). For Western blot, 20 μg of total proteins from cell lysates, or supernatants, were analyzed by 12% SDS/PAGE and blotted onto nitrocellulose membrane

(Schleicher and Schuell and Whatman). Filters were blocked for 90 min at room temperature with 5% nonfat dry milk in tris buffer saline Tween (TBST) buffer (10 mM Tris·HCl, pH 8.0, 0.1% Tween 20, and 150 mM NaCl) and incubated with a 1:2,000 dilution of either anti-NGAL or anti-actin antibodies for 90 min. After TBST washing, blots were incubated for 1 h with HRP-conjugated secondary antibodies (Amersham Biosciences, NXA931), diluted 1:5,000 in TBST buffer, and then revealed by ECL (Amersham Biosciences).

***In vitro* and *In Vivo* Tumorigenicity Assays.** To analyze the ability of the various FRO clones to form colonies in soft agar, 1×10^4 cells were seeded in 60-mm dishes onto 0.3% Noble Agar (Difco) on top of a 0.6% bottom layer. Colonies >50 cells were scored after two weeks of incubation at 37°C. To analyze the ability of the various FRO clones to induce tumor growth in nude mice, 2×10^7 cells were injected s. c. on a flank of each 6-week-old nude mouse (Charles River, Lecco, Italy). Thirty days later, mice were killed and tumors were excised. Tumor weight was determined and their diameters were measured with a caliper. Tumor volume was calculated by the formula: $a^2 \times b \times 0.4$, where a is the smallest diameter and b is the diameter perpendicular to a. No mouse showed signs of wasting or other visible indications of toxicity. The mice were maintained at the Dipartimento di Biologia e Patologia Cellulare e Molecolare animal facility and housed in barrier facilities on a 12 h light dark cycle with food and water available ad libitum. The animal experiments described here were conducted in accordance with accepted standards of animal care and in accordance with the Italian regulations for the welfare of animals used in studies of experimental neoplasia, and the study was approved by our institutional committee on animal care.

Measurement of Apoptosis. A total of 2.5×10^5 cells per well were seeded in six-well culture plates and grown for 24 h at 37°C either in the presence or in the absence of serum. In some cases, cells were grown either in serum-free conditioned medium from FRO cells or in serum-free medium containing human transferrin (10 μg/ml), recombinant NGAL (10 μg/ml), and deferoxamine (200 μg/ml) or $FeCl_3$ (50 μM). Cell death was assessed either by Western blot analysis with an anti-caspase 9 antibody (Stressgen) or by propidium iodide staining according to Nicoletti *et al.* (3). In this case, samples were analyzed by flow cytometry by using a CyAn cytofluoremeter (Dako) equipped with Summit Software. Results were mean ± SD of at least three separate experiments.

mRNA Quantification by Real-time RT-PCR. Real-time RT-PCR was carried out with cDNAs reverse-transcribed from total RNA by using LightCycler-FastStart DNA Master SYBR Green I (Roche) and ABI PRISM 7000 software (Applied Biosystems). The primer used for glyceraldehyde-3-phosphate dehydrogenase was 5′-AAACAGAAGGCAGCTTTACGATG-3′ and 5′-AAATGTTCTGATCCAGTAGCG-3′ for NGAL, and 5′-TCCCAGAGCTGAACGG-3′ and 5′-GAAGTCGCGGAGACA-3′.

Statistics. Data were analyzed with ANOVA and a Student's t test analysis. Data are presented as the means ± SD. P values <0.05 were considered significant.

Chromatin Immunoprecipitation. The cell monolayer of FRO was cross-linked in 1% formaldehyde for 20 min at room temperature. The cross-linking reaction was stopped by adding glycine to a final concentration of 0.125 M and was washed twice in cold PBS containing proteinase inhibitors (Sigma). Cell lysates were prepared and sonicated to afford chromosomal DNA in the range of 400–600 bp. Equal amounts of chromatin lysate were diluted with ChIP dilution buffer to a final volume of 1.0 ml. Twenty microliters of the pre-immunoprecipitated lysate were saved as "input" for later normalization. The chromatin solution was precleared with a salmon sperm DNA/protein A-agarose 50% gel slurry for 1 h at 4°C and immunoprecipitated overnight at 4°C with 5 μg of human α-IκBζ (Santa Cruz, sc-66935; Cell Signaling 9244S), α-p65 (Santa Cruz sc-109, sc-372, sc-7151), α-p50 (Santa Cruz sc-1190, sc-7178), and α-p52 (Santa Cruz sc-7386, sc-298). As a negative control, samples were immunoprecipitated with 5 μg of nonimmune human IgG. After immunoprecipitation, the DNA-histone complex was collected with 40 μl of salmon sperm DNA/protein A-agarose beads for 1 h. Beads were sequentially washed in low salt, high salt, and LiCl and then washed twice with 10 mM Tris, pH 8 and 1 mM EDTA buffers. The DNA-histone complex was then eluted from the beads with 500 μl of $NaHCO_3$/SDS elution buffer. DNA and histones were dissociated at 65°C for 4 h in 5 M NaCl. Proteins were digested by using a proteinase K treatment for 1 h at 45°C. The DNA that had been associated with acetylated histones was extracted by phenol/chloroform/isoamyl alcohol, precipitated with 100% ethanol, and finally resuspended in 20 μl of PCR-grade water and assayed by quantitative real-time PCR. To monitor the relative abundance of promoter that was physically associated with the different transcription factors, DNA samples were used as templates for PCR and had specific primers to amplify a NGAL genomic DNA fragment in the core of the NGAL promoter. The human NGAL gene primers used are forward, 5′-GCAAGATTTCTGCACC-3′, and reverse, 5′-CAAAGGAAGGCACAGAG-3′. PCR was performed by the Sybergreen method by using ABI PRISM 7000 software (Applied Biosystems), and data was calculated by using the ΔCt method ($2^{-\Delta\Delta Ct}$).

Measurement of Mitochondrial Membrane Potential. The changes in mitochondrial membrane potential were quantified by staining cells with tetramethylrhodamine ethyl ester (TMRE) (Invitrogen). A TMRE stock was prepared at a concentration of 10 mg/ml in DMSO and stored at 20°C. Cells were loaded with TMRE by incubating cells in media containing 50 nM TMRE for 30 min at 37°C.

Flow Cytometric Analysis of Cytochrome C Release. Detection of cyt C release was performed as described in ref. 1.

1. Campos C, *et al.* (2006) Method for monitoring of mitochondrial cytochrome c release during cell death: Immunodetection of cytochrome c by flow cytometry after selective permeabilization of the plasma membrane. *Cytometry A*. 69:515–523.
2. Mauro C, *et al.* (2006) ABIN-1 binds to NEMO/IKKgamma and co-operates with A20 in inhibiting NF-kappaB. *J Biol Chem* 281:18482–18488.
3. Nicoletti I, *et al.* (1991) A rapid and simple method for measuring thymocyte apoptosis by propidium iodide staining and flow cytometry. *J Immunol Methods.* 139:271–279.
4. Pacifico F, *et al.* (2007) RbAp48 is a target of nuclear factor-kappaB activity in thyroid cancer. *J Clin Endocrinol Metab* 92:1458–1466.
5. Paron I, *et al.* (2005) A differential proteomic approach to identify proteins associated with thyroid cell transformation. *J Mol Endocrinol* 34(1):199–207.
6. Shevchenko, A *et al.* (1996) Mass spectrometric sequencing of proteins silver-stained polyacrylamide gels. *Anal Chem* 68:850–858.
7. Zhang W, Chait BT (2000) ProFound: An expert system for protein identification by using mass spectrometric peptide mapping information. *Anal Chem* 72:2482–2489.

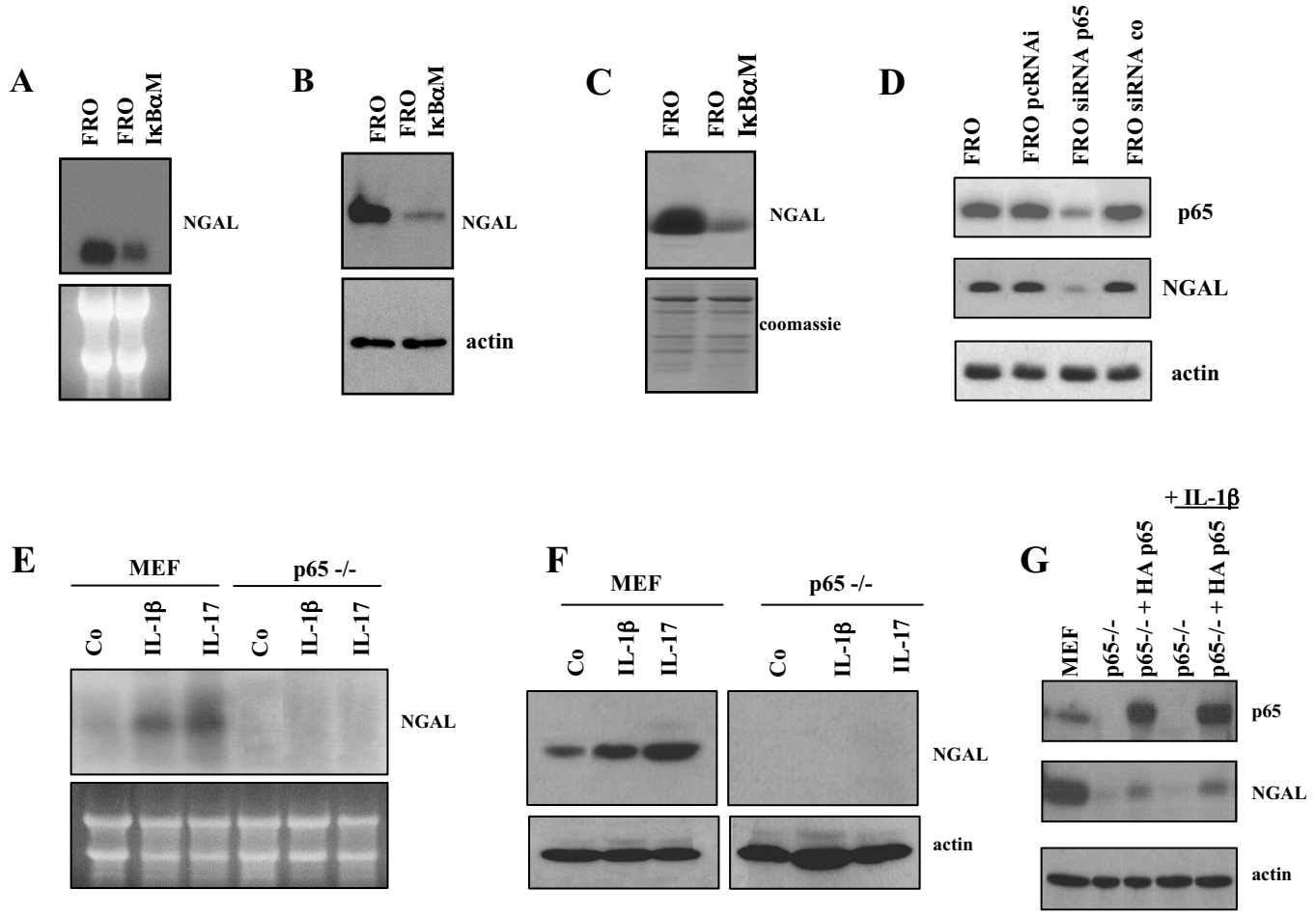

Fig. S1. Analysis of NGAL expression. The different levels of NGAL expression in the FRO and FRO IκBαM cell lines was analyzed by Northern blots (*A Upper*), Western blots on total cell lysates (*B Upper*), and on conditioned media (*C Upper*). The expression levels of NGAL mRNA were normalized to total RNA content (*A Lower*), and those of NGAL protein were normalized to actin expression in cell lysates (*B Lower*) and to Coomassie staining of total protein in conditioned media (*C Lower*). (*D*) Expression of NGAL in FRO cells transiently transfected either with a p65 siRNA (siRNAp65) with the empty vector (pcRNAi) or with an unrelated control siRNA sequence (siRNA co) was determined by Western blot analysis on total cell lysates. Induction of NGAL expression in $p65^{-/-}$ and WT mouse embryonic fibroblasts (MEFs) was analyzed by Northern blot (*E*) and Western blot (*F*). Induction of NGAL expression in $p65^{-/-}$ MEF was reconstituted with an expression vector encoding HA-NGAL (*G*). $p65^{-/-}$ and WT MEFs were treated with either IL1β (20 ng/ml) or IL17 (200 ng/ml) for 6 h.

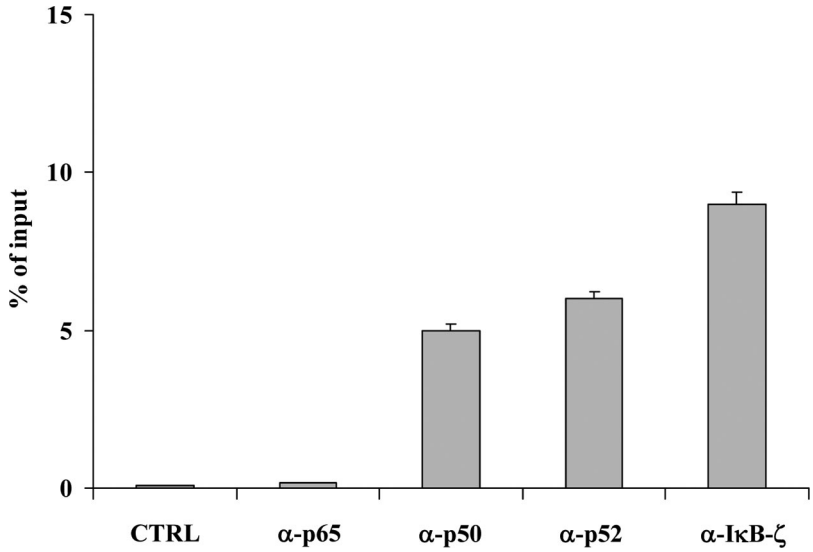

Fig. S2. Chromatin immunoprecipitation. Chromatin from FRO cells, and with the indicated antibodies, was used for ChIP assays. Precipitated DNA for the κB site in the NGAL promoter region was assayed by real-time PCR. Data are representative of three independent experiments.

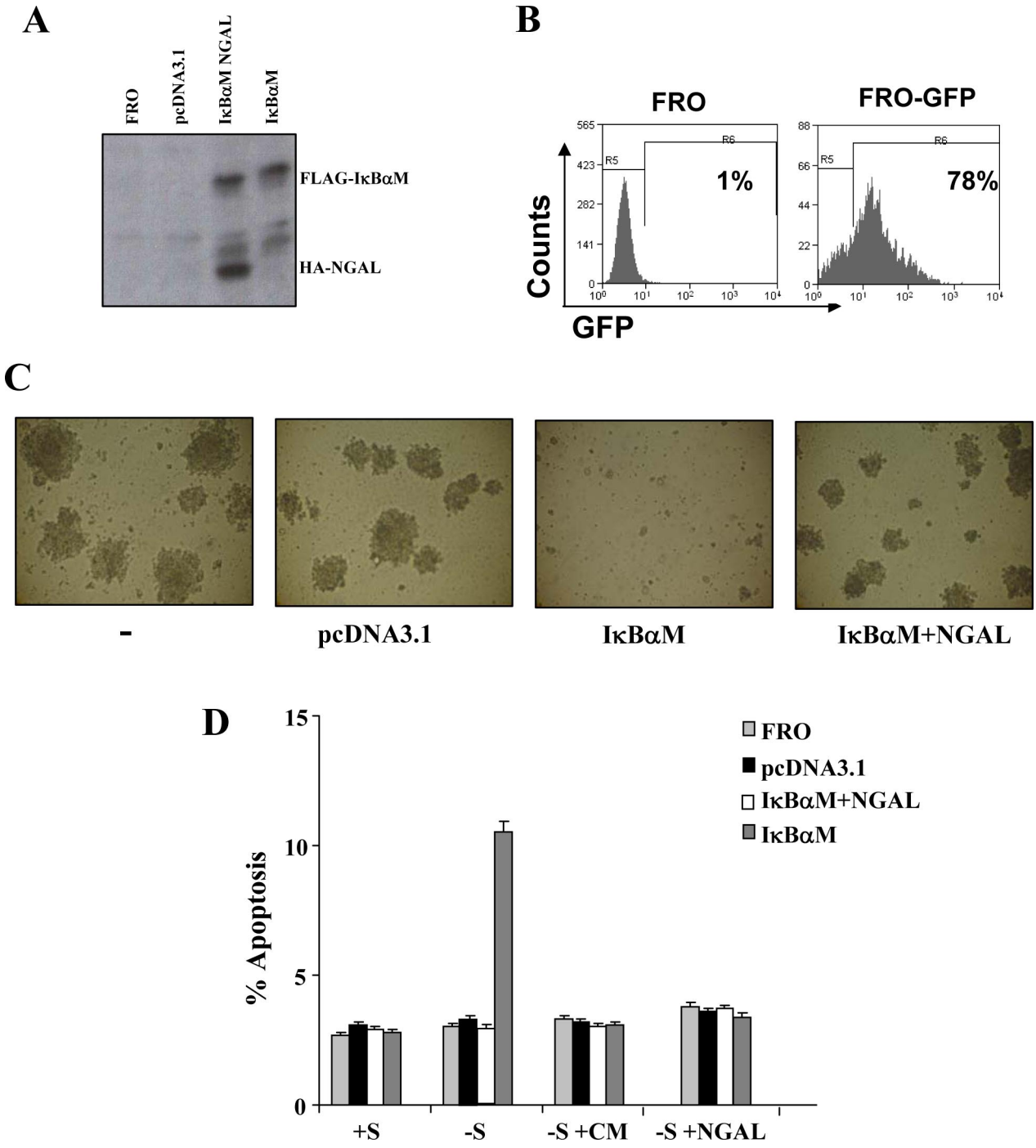

Fig. S3. Effect of NGAL overexpression in FRO IκBαM cells. FRO cells were transiently transfected with an expression vector encoding FLAG tagged IκBαM and with an expression vector encoding HA-tagged NGAL. A vector-encoding GFP was cotransfected to evaluate the transfection efficiency. (*A*) Expression of FLAG-IκBαM and HA-NGAL in the whole cell lysate (both antibodies were used). (*B*) Transfection efficiency was evaluated by FACS. (*C*) Colony formation assay. Colonies >50 cells were scored after 2 weeks of incubation at 37°C. Magnification: ×200. (*D*) 2.5×10^5 cells per well were seeded in 6-well culture plates and grown either in the presence of serum (+*S*), in the absence of serum (−*S*), in serum-free conditioned medium from FRO cells (−*S*+*CM*), or in the presence of recombinant NGAL (+NGAL) for 24 h at 37°C. Cell death was assessed by TMRE staining on GFP positive cells.

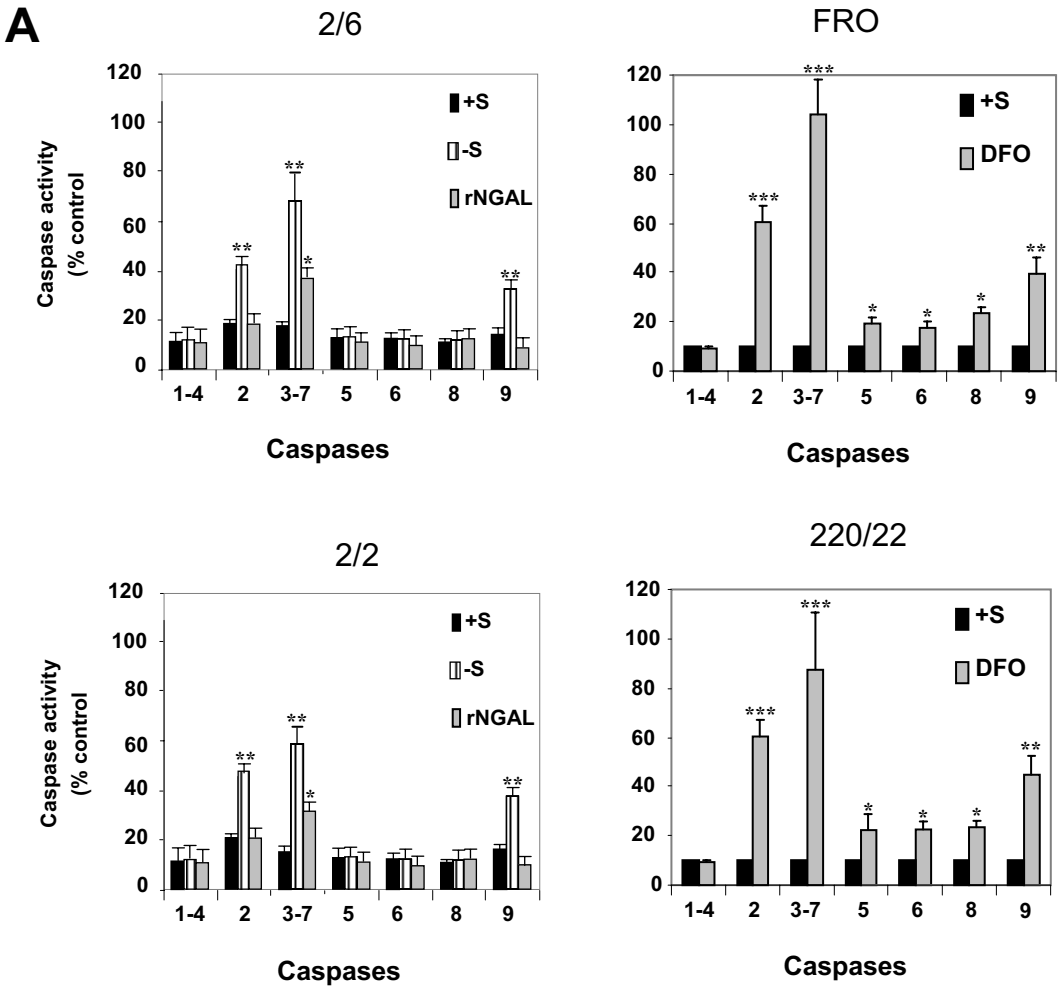

Fig. S4. Analysis of the apoptosis pathways. 2.0×10^6 cells per well were grown in the presence of serum (+*S*), in the absence of serum (−*S*), in serum-free medium containing recombinant NGAL (rNGAL), or in the presence of deferoxamine (DFO) for 24 h at 37°C. Caspase activity was assessed by Caspase Fluorometric Substrate Set Plus (Alexis) (*A*). Mitochondrial membrane potential was assessed by TMRE staining (*B*). Cytocrome C release was assessed by flow cytometry (*C*). *, $P < 0.005$; **, $P < 0.0005$; ***, $P < 0.0001$. In images 2/6 and 2/2, statistical analysis has been performed comparing −S vs. +S, and −S vs. rNGAL. In images FRO and 220/22, statistical analysis has been performed comparing DFO vs. +S.